FUNDAMENTALS OF ADJOINT SENSITIVITIES IN ELECTROMAGNETICS

Natalia K. Nikolova

McMaster University
Department of Electrical and Computer Engineering
Computational Electro-Magnetics Laboratory

Outline

Introduction: Challenges of simulation-based optimization

Background: AVM & self-adjoint sensitivities of *S*-parameters

Point of Interest: Accuracy of an FDFD implementation

Applications: Response gradients in design tuning

Applications: Response gradients in imaging

Introduction: Simulation as Forward Model

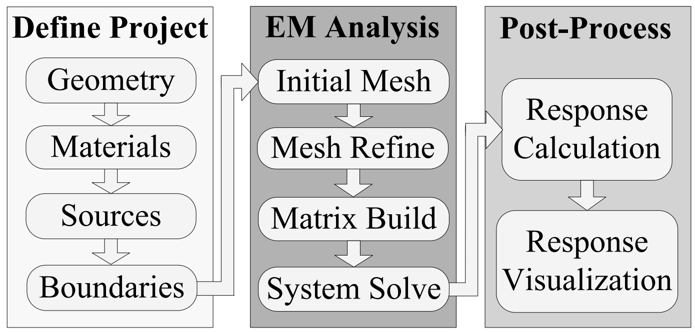

$\mathcal{F}_x : \boldsymbol{p} \rightarrow \boldsymbol{x}$ maps parameters $\boldsymbol{p}$ into field solution $\boldsymbol{x}$

$\mathcal{F}_r : \boldsymbol{p} \rightarrow \boldsymbol{r}$ maps parameters $\boldsymbol{p}$ into responses $\boldsymbol{r}$

$\boldsymbol{p}$ shape and material parameters
$\boldsymbol{x}(\boldsymbol{p})$ field solution
$\boldsymbol{r}(\boldsymbol{x}(\boldsymbol{p}))$ responses

3

Introduction: Simulation-Based Optimization (Design Flowchart)

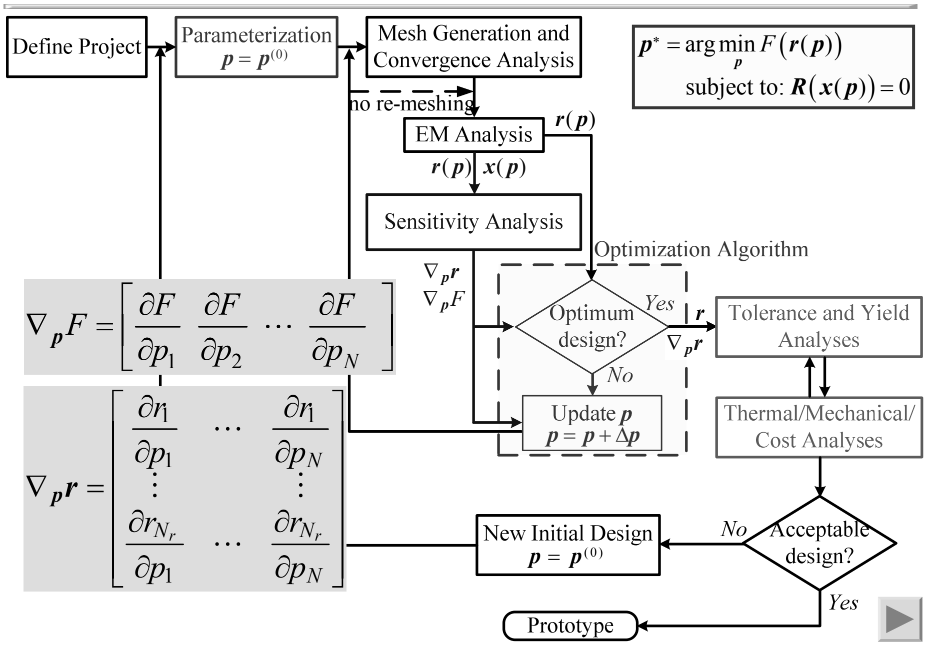

Introduction: Simulation-Based Optimization, cont.

example objective function F – *minimax* formulation

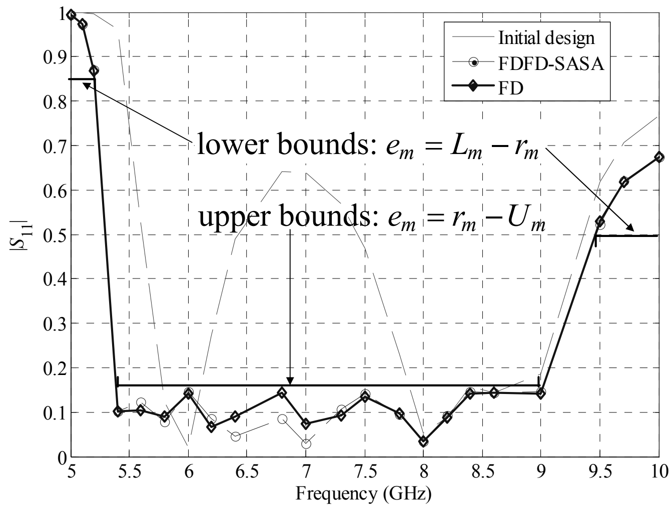

$$\boxed{\begin{array}{l} F = \mathcal{F}(\boldsymbol{e}) \\ \boldsymbol{e} \in \mathbb{R}^{N_r \times 1} \end{array}}$$

$$F = \max\{\boldsymbol{e}\}$$

5

Introduction: Simulation-Based Optimization, cont.

example objective function F – ℓ_2 formulation in imaging

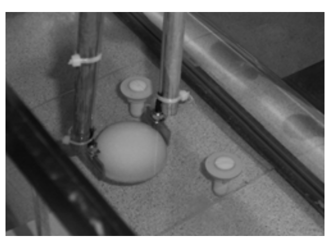

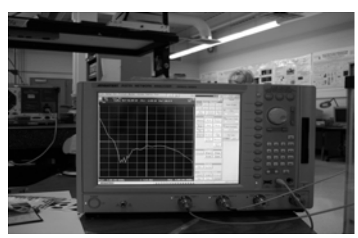

$$F \sim \sum_m e_m^2$$

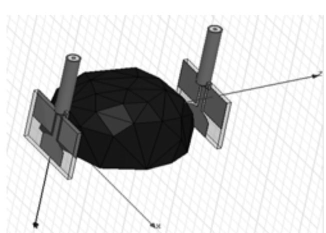

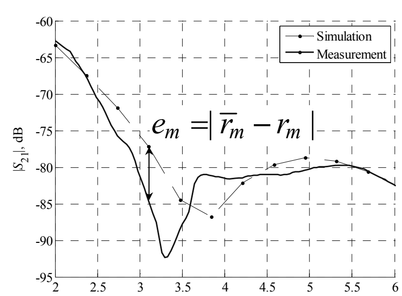

6

Introduction: Pros & Cons of Gradient-based Optimization

fast convergence, i.e., number of iterations is relatively small

overall speed conditional upon Jacobian availability

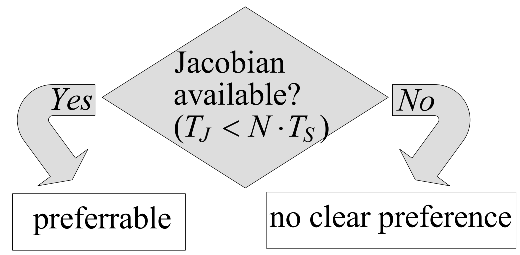

solution is only local (starting point is important)

convergence to a good solution is not guaranteed

gradient-based algorithms preferred in tuning tasks

Challenges in Optimization with Numerical Simulations

- *F* is a strongly nonlinear non-analytical function of ***p***
- optimization problem is not convex
- evaluation of *F* is computationally expensive
- numerical errors are unavoidable – accuracy is limited by resources
- Jacobian is not available
- response-level Jacobian estimates are unreliable and time-consuming
- interfacing external optimization algorithms with commercial EM solvers is fraught with technical complications

Dos and Don’ts in Optimization with Simulators

- determine the accuracy of the simulated responses $\boldsymbol{\delta}$
  - perform mesh convergence analysis $\delta^{(n)} = \| \boldsymbol{r}^{(n+1)} - \boldsymbol{r}^{(n)} \| \leq \boldsymbol{\delta}$
  - typical $\boldsymbol{\delta}$ is about 0.01 for S-parameters of passive devices
- select the values of the termination criteria accordingly
  - objective function: stop if $\Delta F^{(n)} \leq \delta_F$ $\quad \Delta F^{(n)} = \left| F^{(n)} - F^{(n-1)} \right|$
  - $\delta_F \approx | \mathcal{F}(\boldsymbol{\delta u}) |$ $\quad F^{(n)} = \mathcal{F}(\boldsymbol{e}^{(n)})$
  - step in shape-parameter space: stop if $\| \Delta \boldsymbol{p}^{(n)} \| \leq \delta_p$
  - $\delta_p \approx 0.75 l_{\min}$
  - observe termination criteria for 2 or 3 consecutive iterations
- do not change mesh topology from one optimization iteration to another

9

Sensitivity Analysis Based on EM Simulations

objective

$\nabla_p \boldsymbol{r}$ subject to $\boldsymbol{R}(\boldsymbol{x}, \boldsymbol{p}) = \boldsymbol{0}$

Jacobian must be obtained within $T_J << NT_S$

$$\frac{dr}{dp_n} \approx \frac{r(\boldsymbol{p} + \Delta p_n \boldsymbol{u}_n) - r(\boldsymbol{p})}{\Delta p_n}, \; n = 1, \ldots, N$$

response-level finite differences

approach – adjoint variable method

overhead is at the most one additional EM simulation regardless of N

10

Adjoint Variable Method in Electromagnetics

derivatives with respect to parameter p_n, $n = 1,\ldots,N$

system equations

$$\mathbb{L}\mathbf{E} = \mathbf{g}, \quad R(\mathbf{E}) = \mathbb{L}\mathbf{E} - \mathbf{g} = 0$$

$$\Downarrow$$

$$\frac{\partial \mathbb{L}}{\partial p_n}\mathbf{E} + \mathbb{L}\frac{\partial \mathbf{E}}{\partial p_n} = \frac{\partial \mathbf{g}}{\partial p_n}$$

$$\Downarrow$$

$$\left\langle \hat{\mathbf{E}}, \frac{\partial R}{\partial p_n}\mathbf{E} \right\rangle = -\left\langle \hat{\mathbf{E}}, \mathbb{L}\frac{\partial \mathbf{E}}{\partial p_n} \right\rangle$$

$$\frac{\partial R}{\partial p_n} = \frac{\partial \mathbb{L}}{\partial p_n}\bar{\mathbf{E}} - \frac{\partial \mathbf{g}}{\partial p_n}$$

response

$$F(\mathbf{E}) = \iiint_\Omega f(\mathbf{E})\, d\Omega$$

$$\Downarrow$$

$$\frac{\partial F}{\partial p_n} - \frac{\partial^e F}{\partial p_n} = \iiint_\Omega \left(\sum_{\xi = x,y,z} \frac{\partial f}{\partial E_\xi} \cdot \frac{\partial E_\xi}{\partial p_n} \right) d\Omega$$

$$\Downarrow$$

$$\frac{\partial F}{\partial p_n} - \frac{\partial^e F}{\partial p_n} = \left\langle \frac{\partial \mathbf{E}}{\partial p_n}, \hat{\mathbf{g}} \right\rangle$$

$$\hat{\mathbf{g}} = \sum_{\xi = x,y,z} \frac{\partial f}{\partial E_\xi}\hat{\mathbf{a}}_\xi$$

11

AVM in Electromagnetics, cont.

the "transpose" (or pseudo-adjoint) of the EM operator is the one where the constitutive tensors are $\boldsymbol{\varepsilon}^T$ and $\boldsymbol{\mu}^T$

$$\langle \mathbf{f}, \mathbb{L}\mathbf{g} \rangle = \langle \mathbf{g}, \mathbb{L}^T \mathbf{f} \rangle$$

system equations

$$\vdots$$

$$\left\langle \hat{\mathbf{E}}, \frac{\partial R}{\partial p_n}\mathbf{E} \right\rangle = -\left\langle \hat{\mathbf{E}}, \mathbb{L}\frac{\partial \mathbf{E}}{\partial p_n} \right\rangle$$

$$\Downarrow$$

$$\left\langle \hat{\mathbf{E}}, \frac{\partial R}{\partial p_n}\mathbf{E} \right\rangle = -\left\langle \frac{\partial \mathbf{E}}{\partial p_n}, \underbrace{\mathbb{L}^T \hat{\mathbf{E}}}_{\hat{\mathbf{g}}} \right\rangle$$

response

$$\vdots$$

$$\frac{\partial F}{\partial p_n} - \frac{\partial^e F}{\partial p_n} = \left\langle \frac{\partial \mathbf{E}}{\partial p_n}, \hat{\mathbf{g}} \right\rangle$$

$$\frac{\partial F}{\partial p_n} = \frac{\partial^e F}{\partial p_n} - \iiint_\Omega \hat{\mathbf{E}} \cdot \frac{\partial R(\bar{\mathbf{E}})}{\partial p_n} d\Omega$$

$$\boxed{\mathbb{L}^T \hat{\mathbf{E}} = \hat{\mathbf{g}}}$$

12

AVM in Electromagnetics: Implementation with FDFD

$$\frac{\partial F}{\partial p_n} = \frac{\partial^e F}{\partial p_n} - \iiint_\Omega \hat{\mathbf{E}} \cdot \frac{\partial R(\bar{\mathbf{E}})}{\partial p_n} d\Omega \qquad \boxed{\mathbb{L}^T \hat{\mathbf{E}} = \hat{\mathbf{g}}}$$

$$\mathbb{L}\mathbf{E} = \mathbf{g}, \quad R(\mathbf{E}) = \mathbb{L}\mathbf{E} - \mathbf{g} = 0$$

assume residual R uses a FDFD model based on Helmholtz equation

$$R(\mathbf{E}) = \nabla \times \tilde{\boldsymbol{\mu}}_r^{-1} \nabla \times \mathbf{E} - k_0^2 \tilde{\boldsymbol{\varepsilon}}_r \mathbf{E} + j\omega\mu_0 \mathbf{J} = 0$$

source term

after FD discretization

$$\Rightarrow C^2\mathbf{E} + \alpha\mathbf{E} - \mathbf{G} = 0$$

$$C^2 \approx -\nabla \times \boldsymbol{\mu}_r^{-1} \nabla \times$$

$$\alpha = k_0^2 \left[\varepsilon_r - j\varepsilon_r \tan\delta_d - j\sigma(\omega\varepsilon_0)^{-1} \right]$$

$$\mathbf{G} = j\omega\mu_0 \mathbf{J}$$

13

AVM in Electromagnetics: Implementation with FDFD, cont.

the double-curl operator is discretized using central-node FD grid

$$C^2 \approx -\nabla \times \boldsymbol{\mu}_r^{-1} \nabla \times$$

x-component

$x \to y \to z \to x$

$$(C^2\mathbf{E})_x = \frac{D_{yy}^\mu E_x}{\Delta y^2} + \frac{D_{zz}^\mu E_x}{\Delta z^2} - \frac{D_{yx}^\mu E_y}{\Delta y \Delta x} - \frac{D_{zx}^\mu E_z}{\Delta z \Delta x}$$

$$(D_{yy}^\mu E_x)_{(x_0,y_0,z_0)} = \frac{E_{x(x_0,y_0+\Delta y,z_0)}}{\tilde{\mu}_{r(x_0,y_0+\Delta y/2,z_0)}} + \frac{E_{x(x_0,y_0-\Delta y,z_0)}}{\tilde{\mu}_{r(x_0,y_0-\Delta y/2,z_0)}} - \left[\frac{1}{\tilde{\mu}_{r(x_0,y_0+\Delta y/2,z_0)}} + \frac{1}{\tilde{\mu}_{r(x_0,y_0-\Delta y/2,z_0)}} \right] \cdot E_{x(x_0,y_0,z_0)}$$

$$(D_{yx}^\mu E_y)_{(x_0,y_0,z_0)} = \frac{1}{4} \left[\frac{E_{y(x_0+\Delta x,y_0+\Delta y,z_0)} - E_{y(x_0-\Delta x,y_0+\Delta y,z_0)}}{\tilde{\mu}_{r(x_0,y_0+\Delta y,z_0)}} - \frac{E_{y(x_0+\Delta x,y_0-\Delta y,z_0)} - E_{y(x_0-\Delta x,y_0-\Delta y,z_0)}}{\tilde{\mu}_{r(x_0,y_0-\Delta y,z_0)}} \right].$$

14

AVM in Electromagnetics: Implementation with FDFD, cont.

linear operator and source term $\mathbb{L} = C^2 + \alpha,\ \mathbf{g} = \mathbf{G}$

residual derivative

$$\frac{\partial R(\overline{\mathbf{E}})}{\partial p_n} = \frac{\partial \mathbb{L}}{\partial p_n}\overline{\mathbf{E}} - \frac{\partial \mathbf{g}}{\partial p_n}$$

$$\frac{\partial R(\overline{\mathbf{E}})}{\partial p_n} = \frac{\partial C^2\overline{\mathbf{E}}}{\partial p_n} + \frac{\partial \alpha}{\partial p_n}\overline{\mathbf{E}} - \frac{\partial \mathbf{G}}{\partial p_n}$$

usually zero

derivatives of system coefficients *wrt* material parameters

$$\frac{\partial C^2\overline{\mathbf{E}}}{\partial \tilde{\mu}_r} = \begin{cases} -\dfrac{C^2\overline{\mathbf{E}}}{\tilde{\mu}_r}, & \text{if } p_n = \mu_r \\ 0, & \text{if } p_n = \sigma \text{ or } \tan\delta_d \end{cases} \qquad \frac{\partial \alpha}{\partial p_n} = \begin{cases} k_0^2(1 - j\tan\delta_d), & \text{if } p_n = \varepsilon_r \\ -j\dfrac{k_0^2}{\omega\varepsilon_0}, & \text{if } p_n = \sigma \\ -j\varepsilon_r k_0^2, & \text{if } p_n = \tan\delta_d \end{cases}$$

15

AVM in Electromagnetics: Implementation with FDFD, cont.

summary of exact sensitivity analysis with the FDFD method

$$\frac{\partial F}{\partial p_n} = \frac{\partial^e F}{\partial p_n} - \iiint_\Omega \hat{\mathbf{E}} \cdot \frac{\partial R(\overline{\mathbf{E}})}{\partial p_n} d\Omega$$

where

$$\frac{\partial R(\overline{\mathbf{E}})}{\partial p_n} = \frac{\partial C^2\overline{\mathbf{E}}}{\partial p_n} + \frac{\partial \alpha}{\partial p_n}\overline{\mathbf{E}}$$

and the adjoint field is the solution of

$$\mathbb{L}^T\hat{\mathbf{E}} = \hat{\mathbf{g}}, \quad \hat{\mathbf{g}} = \sum_{\xi = x,y,z} \frac{\partial f}{\partial E_\xi}\hat{\mathbf{a}}_\xi$$

this formula is directly applicable with material parameters

16

AVM in Electromagnetics: Implementation with FDFD, cont.

[Nikolova, Zhu, Song, Hasib, and Bakr, *IEEE Trans. Microwave Theory Tech.*, June 2009]

approximate sensitivity analysis for shape parameters (FDFD method)

$$\frac{\partial F}{\partial p_n} \approx \frac{\partial^e F}{\partial p_n} - \iiint_{\Omega} \hat{\mathbf{E}}_n \cdot \frac{\Delta R(\overline{\mathbf{E}})}{\Delta p_n} d\Omega$$

where

$$\frac{\Delta R(\overline{\mathbf{E}})}{\Delta p_n} = \frac{\Delta C^2 \overline{\mathbf{E}}}{\Delta p_n} + \frac{\Delta \alpha}{\Delta p_n} \cdot \overline{\mathbf{E}} - \frac{\Delta(j\omega\mu_0 \mathbf{J}^{\text{ind}})}{\Delta p_n}$$

and the adjoint field is the solution of the perturbed adjoint problem

$$\mathbb{L}_n^T \hat{\mathbf{E}}_n = \hat{\mathbf{g}}, \quad \hat{\mathbf{g}} = \sum_{\xi = x,y,z} \frac{\partial f}{\partial E_\xi} \hat{\mathbf{a}}_\xi$$

17

AVM in Electromagnetics: Implementation with MoM

[Georgieva, Glavic, Bakr, and Bandler, *IEEE Trans. Microwave Theory Tech.*, Dec. 2002]

the linear EM problem in matrix form

$$\boldsymbol{ZI} = \boldsymbol{V} \quad \Leftrightarrow \quad \mathbb{L}\boldsymbol{x} = \mathbf{g} \ \text{ or } \ \boldsymbol{R}(\boldsymbol{x}) = \mathbb{L}\boldsymbol{x} - \mathbf{g} = 0$$

$$\Rightarrow \mathbb{L} = \boldsymbol{Z} \text{ and } \boldsymbol{g} = \boldsymbol{V} \ \Rightarrow \ \boldsymbol{R}(\overline{\boldsymbol{I}}) = \boldsymbol{Z}\overline{\boldsymbol{I}} - \boldsymbol{V}$$

$\boldsymbol{Z}(\boldsymbol{p})$ system matrix

$\boldsymbol{I} = [i_1 \ldots i_M]^T$ state variable vector (solution)

$\boldsymbol{V} = [v_1 \ldots v_M]^T$ excitation vector

$\boldsymbol{p} = [p_1 \ \cdots \ p_N]^T$ design variables

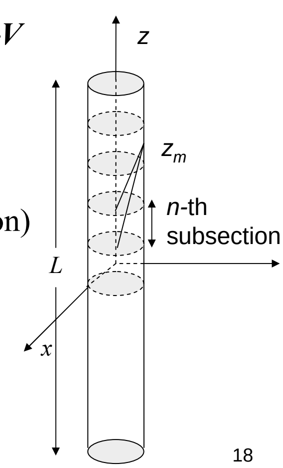

18

AVM in Electromagnetics: Implementation with MoM

exact sensitivity formula for linear deterministic problems in matrix form

$$\frac{\partial F}{\partial p_n} = \frac{\partial^e F}{\partial p_n} - \left\langle \hat{\boldsymbol{I}}, \frac{\partial R(\bar{\boldsymbol{I}})}{\partial p_n} \right\rangle \qquad \frac{\partial \boldsymbol{R}(\bar{\boldsymbol{I}})}{\partial p_n} = \frac{\partial \boldsymbol{Z}}{\partial p_n}\bar{\boldsymbol{I}} - \underbrace{\frac{\partial \boldsymbol{V}}{\partial p_n}}_{\text{usually zero}}$$

$$\boxed{\frac{\partial F}{\partial p_n} = \frac{\partial^e F}{\partial p_n} + \hat{\boldsymbol{I}}^T \cdot \left(\frac{\partial \boldsymbol{V}}{\partial p_n} - \frac{\partial \boldsymbol{Z}}{\partial p_n}\bar{\boldsymbol{I}} \right), \quad n = 1, \ldots, N}$$

where

$$\boldsymbol{Z}^T \hat{\boldsymbol{I}} = \left[\nabla_{\boldsymbol{I}} F \right]^T_{\boldsymbol{I}=\bar{\boldsymbol{I}}}$$

S-parameter Self-adjoint Sensitivity Analysis

[Nikolova, Zhu, Song, Hasib, and Bakr, *IEEE Trans. Microwave Theory Tech.*, June 2009]

S-parameters as functionals of the **E**-field at the ports

$$S_{kj}^{(\upsilon)} = \frac{\iint_{S_k} (\mathbf{E}_j \times \mathbf{h}_k^{(\upsilon)}) \cdot d\mathbf{s}}{\iint_{S_j} (\mathbf{E}_j^{\text{inc}} \times \mathbf{h}_j^{(\upsilon)}) \cdot d\mathbf{s}} - \delta_{kj}, \quad \delta_{kj} = \begin{cases} 1, & k = j \\ 0, & k \neq j \end{cases} \qquad S_{kj}^{(\upsilon)} = \frac{F_{kj}}{V_j} - \delta_{kj}$$

$$k, j = 1, \ldots, K$$

assume ports do not depend on ***p***

modal vectors and magnitudes are then independent of ***p***

modal vectors

$$\iint_{S_\varsigma} \left(\mathbf{e}_\varsigma^{(\upsilon)} \times \mathbf{h}_\varsigma^{(\upsilon')} \right) \cdot d\mathbf{s} = \begin{cases} 1, & \text{if } \upsilon = \upsilon' \\ 0, & \text{if } \upsilon \neq \upsilon' \end{cases}$$

modal incident-wave magnitude

$$V_j = \iint_{S_j} (\mathbf{E}_j^{\text{inc}} \times \mathbf{h}_j^{(\upsilon)}) \cdot d\mathbf{s}$$

S-parameter Self-adjoint Sensitivity Analysis, cont.

the generalized response

$$F(\mathbf{E}) = \iiint_{\Omega} f(\mathbf{E})d\Omega + \oiint_{S_\Omega} f_s(\mathbf{E})ds$$

in the case of S-parameters, $F = F_{kj}$ $\quad F_{kj} = \iint_{S_k} (\mathbf{E}_j \times \mathbf{h}_k^{(\upsilon)}) \cdot d\mathbf{s}$

$$f = 0 \text{ and } f_s = \begin{cases} (\mathbf{E}_j \times \mathbf{h}_k^{(\upsilon)}) \cdot \mathbf{a}_n, \text{ at } S_k \\ 0, \text{ elsewhere on } S_\Omega \end{cases}$$

excitation via port boundary (no volume sources!)

$$\mathbb{L}\mathbf{E} = 0 \qquad \mathbb{L}^T \hat{\mathbf{E}} = 0$$

if $\boldsymbol{\varepsilon}^T = \boldsymbol{\varepsilon}$ and $\boldsymbol{\mu}^T = \boldsymbol{\mu}$, the EM operator is symmetric

[Chew *et al.*, *Integral Equation Methods for Electromagnetic and Elastic Waves*, 2008]

$$\mathbb{L}^T = \mathbb{L} \quad \Rightarrow \quad \mathbb{L}\hat{\mathbf{E}} = 0$$

21

S-parameter Sensitivity Analysis, cont.

adjoint field can be obtained from the **E**-field – no need for adjoint system analyses!

how? – set boundary conditions in adjoint problem same as in original problem, incl. those at excitation ports

adjoint field for F_{kj} turns out to be linearly dependent (in a complex sense) on the original field $\mathbf{E}_k$

$$\hat{\mathbf{E}}_{kj} = \kappa_{kj}\overline{\mathbf{E}}_k, \ \kappa_{kj} = -(2V_k j\omega\mu_0)^{-1}$$

exact sensitivity formula for S_{kj}

$$\frac{\partial S_{kj}}{\partial p_n} = \frac{1}{2V_k V_j j\omega\mu_0} \iiint_{\Omega} \overline{\mathbf{E}}_k \cdot \frac{\partial R(\overline{\mathbf{E}}_j)}{\partial p_n} d\Omega$$

22

S-parameter Sensitivity Analysis, cont.

sensitivity formula for shape parameters

$$\frac{\partial S_{kj}}{\partial p_n} = \frac{1}{2V_k V_j j\omega\mu_0} \iiint_{\Omega} \overline{\mathbf{E}}_k \cdot \frac{\Delta_n R(\overline{\mathbf{E}}_j)}{\Delta p_n} d\Omega$$

implementation involves assumed perturbations in both forward and backward directions of one cell size

Memory Requirements: Recording the Field

field is recorded at voxels whose material parameters change as a result of an assumed parameter perturbation

shape parameters

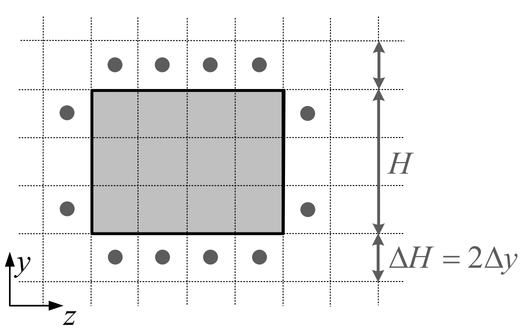

material parameters

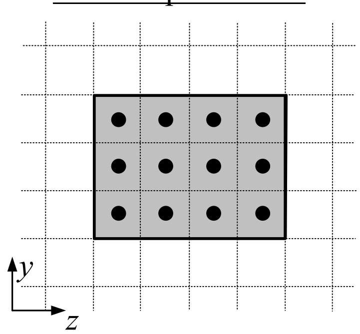

Algorithm for the Self-adjoint *S*-parameter Sensitivity Calculation

parameterization: determine optimizable parameters

generate local FD sensitivity grids at optimizable objects

calculate derivatives of system coefficients

acquire **E**-field solution at sensitivity-grid points at all frequencies

acquire or calculate modal magnitudes at ports

calculate sensitivity integral

25

Accuracy of Self-adjoint *S*-parameter Sensitivities

dielectric-post bandstop filter **[Minakova and Rud, 2000]**

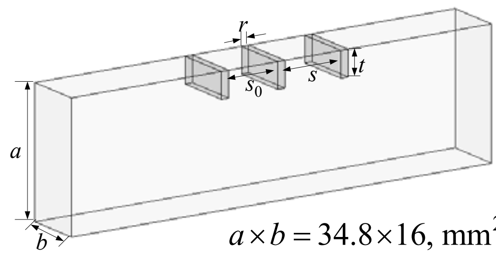

$r_0 = 2.088$, mm
$t_0 = 6.960$, mm
$s_0 = 14.0$, mm
$\varepsilon_r = 38.5$

$a \times b = 34.8 \times 16$, mm^2

S-parameter error

$$e_p = |S_{11}|^2 + |S_{21}|^2 - 1$$

S-parameter derivative error

$$e_d = 2|S_{11}| \cdot \frac{\partial |S_{11}|}{\partial p_n} + 2|S_{21}| \cdot \frac{\partial |S_{21}|}{\partial p_n} = 0$$

26

Accuracy of Self-adjoint *S*-parameter Sensitivities, cont.

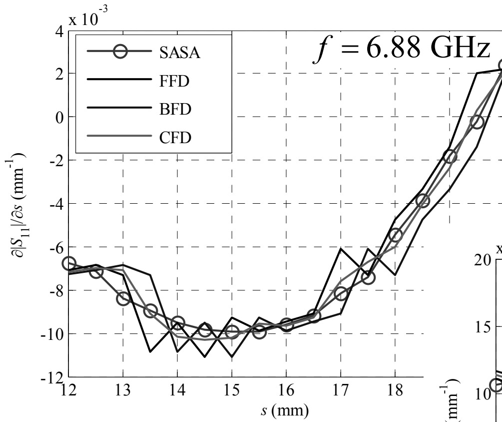

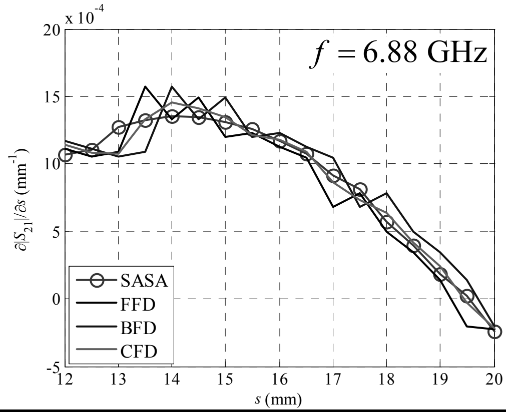

response-level FD estimates

$\Delta s = 0.5$, mm

sensitivity-grid step

$\Delta h = r_0 / 4 = 0.522$, mm

Accuracy of Self-adjoint *S*-parameter Sensitivities, cont.

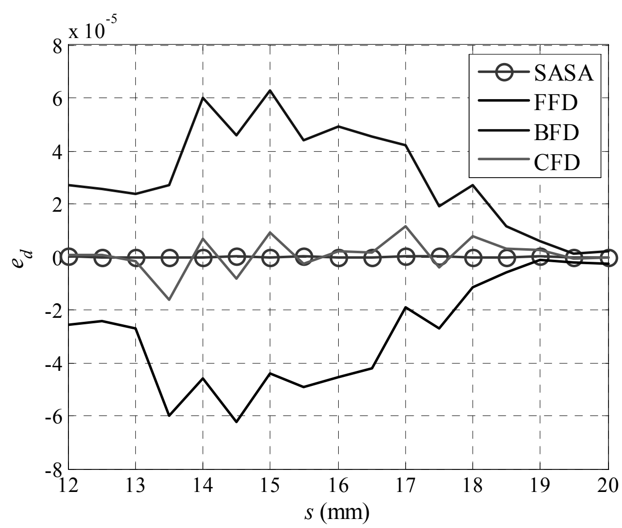

$(e_d)_{\text{SASA}} \sim 10^{-9}$

$(e_d)_{\text{CFD}} \sim 10^{-5}$

$e_p \sim 10^{-8}$

28

Accuracy of Self-adjoint *S*-parameter Sensitivities, cont.

two-section waveguide impedance transformer **[Young, 1960]**

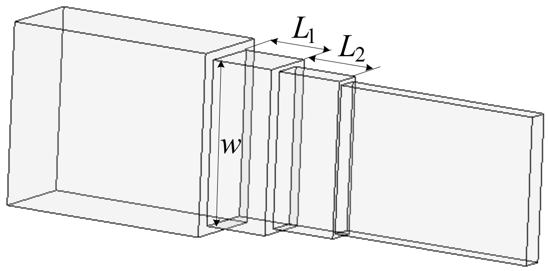

nominal cross-sections

42×21, mm^2

38×14, mm^2

36×7, mm^2

34×5, mm^2

nominal lengths

$L_1 = 15.2$, mm

$L_2 = 15.6$, mm

Accuracy of Self-adjoint *S*-parameter Sensitivities, cont.

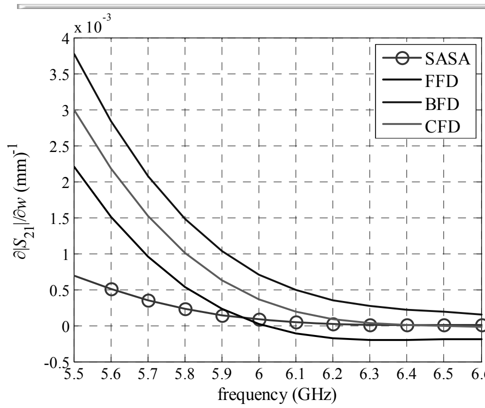

response-level FD estimates

$\Delta w = 1.0$, mm

sensitivity-grid step

$\Delta h = 2.0$, mm

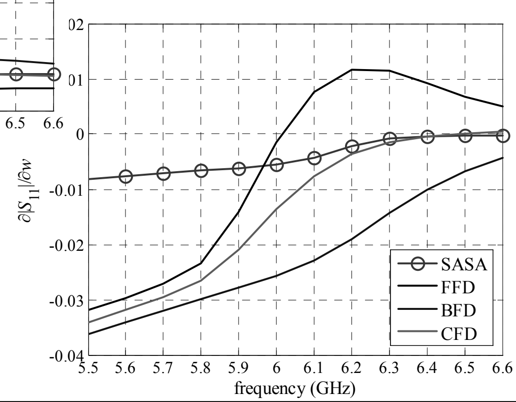

Accuracy of Self-adjoint *S*-parameter Sensitivities, cont.

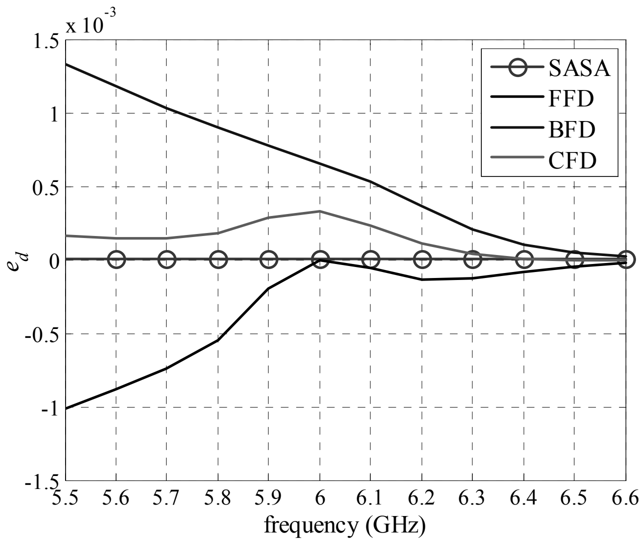

$(e_d)_{\text{SASA}} \sim 10^{-8}$

$(e_d)_{\text{CFD}} \sim 10^{-4}$

$e_p \sim 10^{-7}$

31

Applications in Design Tuning: Dielectric-resonator Antenna

[Yau and Shuley, 1999]

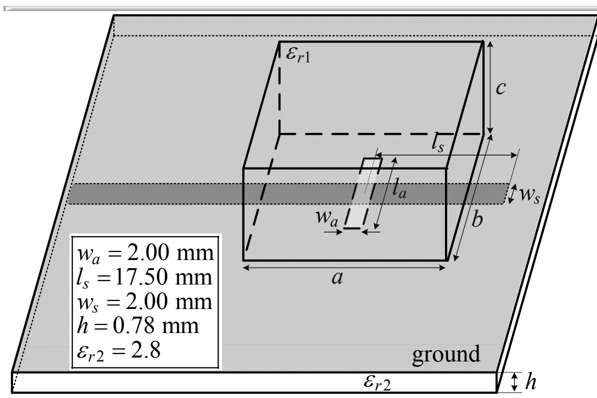

$\boldsymbol{p}^T = [\varepsilon_{r1}\;\; a\;\; b\;\; c\;\; l_a]$

$\boldsymbol{p}^{(0)} = [12\;\; 23\;\; 23\;\; 10\;\; 20]^T$

[all lengths in mm]

<u>optimization setup</u> (Jacobians: SASA, FFD 4%)

optimizer: *minimax* **[Bandler, Kellerman, Madsen, 1985]**

initial trust region radius: $r^{(0)} = 0.01\|\boldsymbol{p}^{(0)}\|$

termination criterion:

$$\Delta_p^{(k)} = \frac{\|\boldsymbol{p}^{(k+1)} - \boldsymbol{p}^{(k)}\|}{\|\boldsymbol{p}^{(k)}\|}$$

$$\Delta_F^{(k)} = \|F^{(k+1)} - F^{(k)}\|$$

$$(\Delta_p^{(k)} \le \delta_p \,.\text{and}.\, \Delta_p^{(k-1)} \le \delta_p) \,.\text{or}.\, (\Delta_F^{(k)} \le \delta_F \,.\text{and}.\, \Delta_F^{(k-1)} \le \delta_F)$$

$\delta_p = 0.013$

$\delta_F = 0.010$

Applications in Design Tuning: Dielectric-resonator Antenna, cont.

specs, initial design and final designs

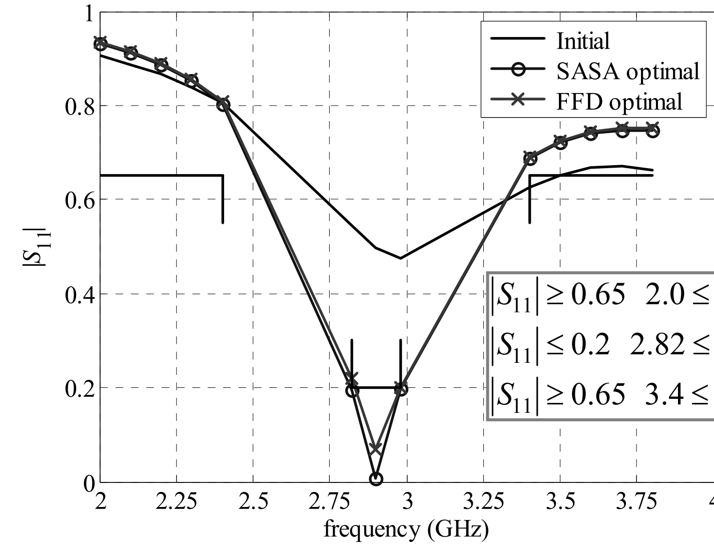

$|S_{11}| \geq 0.65 \quad 2.0 \leq f \leq 2.4$ GHz

$|S_{11}| \leq 0.2 \quad 2.82 \leq f \leq 2.98$ GHz

$|S_{11}| \geq 0.65 \quad 3.4 \leq f \leq 3.8$ GHz .

33

Applications in Design Tuning: Dielectric-resonator Antenna, cont.

summary of optimization processes

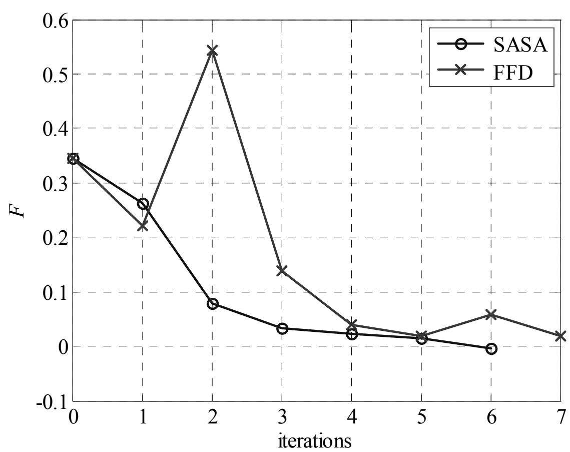

$$\Delta \boldsymbol{p}_{\text{FFD}} = \begin{bmatrix} 0.5 \\ 0.04a \\ 0.04b \\ 0.05c \\ 0.05l_a \end{bmatrix}$$

<u>stops when</u>

SASA opt: $\Delta_F^{(k)} \leq 0.01$

FFD opt: $\Delta_p^{(k)} \leq 0.013$

reducing δ_p does not help FFD opt

$$p^*_{\text{SASA}} = \begin{bmatrix} 10.06 & 23.66 & 23.47 & 13.64 & 17.46 \end{bmatrix}^T$$

$$p^*_{\text{FFD}} = \begin{bmatrix} 10.59 & 23.58 & 23.21 & 12.74 & 17.21 \end{bmatrix}^T$$

34

Applications in Design Tuning: Dielectric-resonator Antenna, cont.

CPU time comparison (per optimization iteration)

HFSS frequency sweep: 220 s
SASA Jacobian calculation: 0.1 s
FFD Jacobian calculation: 1100 s

<u>TOTAL</u>
SASA opt: 1321 s
FFD opt: 9240 s

Applications in Design Tuning: Dielectric-resonator Filter

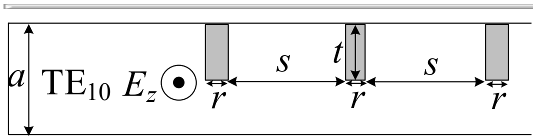

$a \times b = (34.8 \times 8)\ \text{mm}^2$
$\boldsymbol{p} = [t \quad r \quad s]^T \quad \varepsilon_r = 38.5$
$\boldsymbol{p}^{(0)} = [5.5\ \ 2.0\ \ 14]^T$ mm

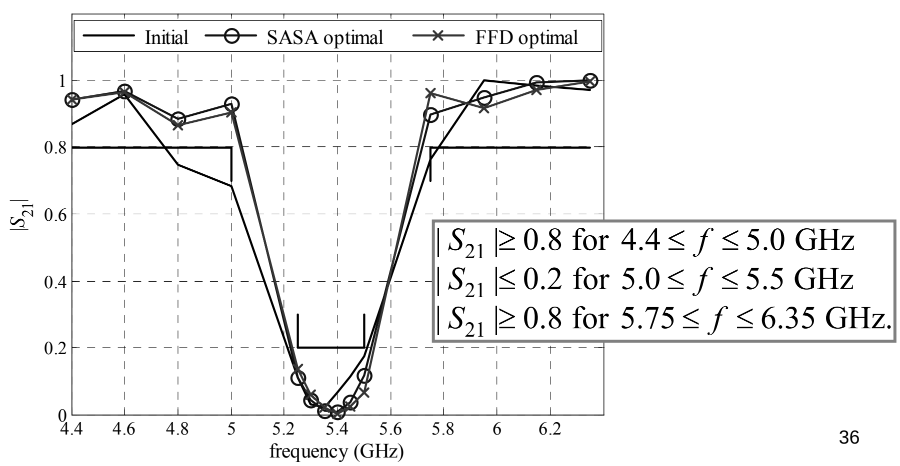

Applications in Design Tuning: Dielectric-resonator Filter, cont.

minimax optimization process

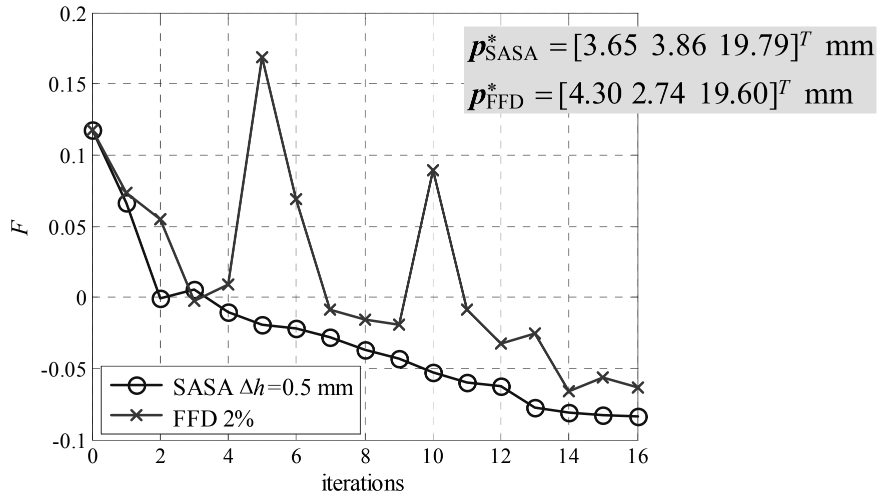

37

Applications in Design Tuning: Dielectric-resonator Filter, cont.

CPU time comparison (per optimization iteration)

HFSS frequency sweep: 459 s
SASA Jacobian calculation: 0.45 s
FFD Jacobian calculation: 1377 s

reliability comparison

$\boldsymbol{p}^{(0)} = [7.5\ \ 1.5\ \ 13.5]^T$ mm

FFD 2%: does not converge, $F = 0.2330$
SASA: converges after 20 iterations, $F = -0.0677$

38

Applications in Design Tuning: H-plane Filter

$\delta = 0.6223$ mm
$S_1 = S_2 = 16.18$ mm
$S_3 = 16.80$ mm

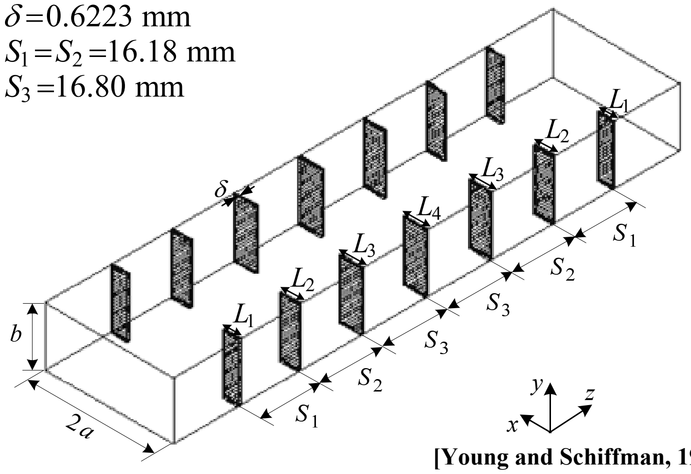

[Young and Schiffman, 1963]

values for termination criterion

$$\delta_p = 0.001$$
$$\delta_F = 0.009$$

$$\boldsymbol{p} = [L_1 \;\; L_2 \;\; L_3 \;\; L_4]^T$$
$$\boldsymbol{p}^{(0)} = [5\delta \;\; 11\delta \;\; 9\delta \;\; 13\delta]^T$$

39

Applications in Design Tuning: H-plane Filter, cont.

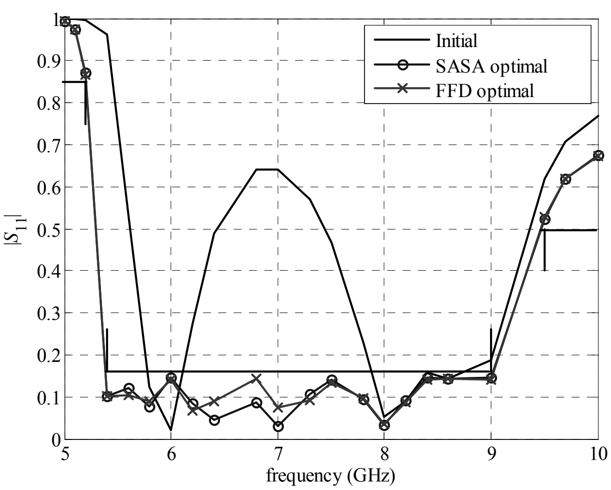

$$|S_{11}| \geq 0.85 \quad f \leq 5.2 \text{ GHz}$$
$$|S_{11}| \leq 0.16 \quad 5.4 \leq f \leq 9 \text{ GHz}$$
$$|S_{11}| \geq 0.5 \quad f \geq 9.5 \text{ GHz}$$

40

Applications in Design Tuning: H-plane Filter, cont.

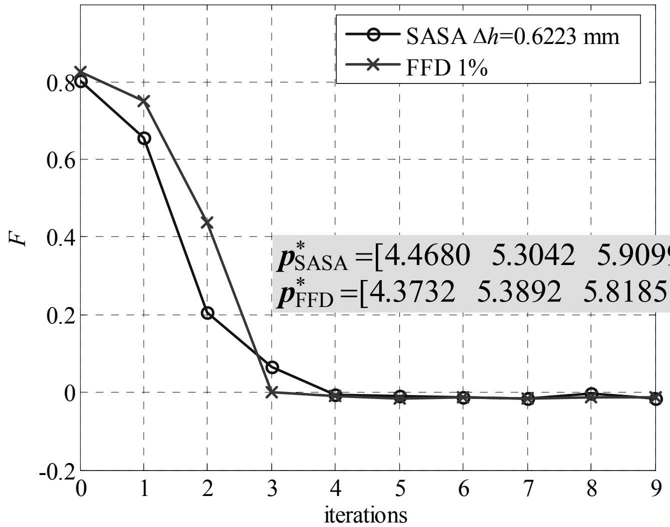

$\boldsymbol{p}^*_{\text{SASA}} = [4.4680 \quad 5.3042 \quad 5.9099 \quad 5.9024]^T$
$\boldsymbol{p}^*_{\text{FFD}} = [4.3732 \quad 5.3892 \quad 5.8185 \quad 5.9821]^T$
[in mm]

41

Applications in Design Tuning: H-plane Filter, cont.

time comparison

	FFD	SASA
number of iterations	10	10
calls to the simulator	50	10
time for 1 simulation (s)	537	537
Jacobian estimation, total (s)	21 480	1 536 (CPU time ≈ 4 s)
total optimization time (s)	32 063	7 216

42

Applications in Microwave UWB Imaging

applications of near-field microwave imaging

- cancer diagnostics (microwave tomography)
- nondestructive testing for structural integrity
- concealed weapon detection
  - etc.

near-field UWB imaging with EM simulations as forward models

- medium is complex
- exploits near-zone (evanescent) field information
- exploits multi-frequency information
- exploits co- and cross-polarization scatter
- solved as a ***nonlinear optimization problem***

43

Objective Functions in Microwave Imaging, cont.

typical number of optimizable parameters N is 10^4 to 10^5 (permittivity and conductivity of each voxel in the imaged volume)

stochastic optimization approaches are impractical – gradient-based approaches are preferred if Jacobians are available

response-level Jacobian approximations are not possible

adjoint Jacobians do not suffer from accuracy and time limitations (may increase memory requirements in time-domain simulations)

minima of 3-D Jacobian maps point directly to possible scatterer locations

44

Objective Function in Microwave Imaging

$$F(\boldsymbol{\varepsilon},\boldsymbol{\sigma}) = \sum_{i=1}^{N_r} (r_i - \overline{r}_i)^2 + \rho_\varepsilon \sum_{n=1}^{N} |\, \varepsilon_n - \varepsilon_{bn} \,|^2 + \rho_\sigma \sum_{n=1}^{N} |\, \sigma_n - \sigma_{bn} \,|^2$$

set regularization terms to 0

$\boldsymbol{r} \in \mathbb{R}^{N_r \times 1}$

$\boldsymbol{\varepsilon},\boldsymbol{\sigma} \in \mathbb{R}^{N \times 1}$

two types of responses are derived from S-parameters
[Li, Trehan and Nikolova, *Inverse Problems*, 2010]

- magnitude response

$$F_{\mathrm{M}}^{(i)}(\tilde{\boldsymbol{\varepsilon}}) = 0.5 \sum_{j,k=1}^{K} \left(|\, S_{kj}^{(i)} \,| - |\, \overline{S}_{kj}^{(i)} \,| \right)^2 \qquad i = 1,\ldots,N_f$$

- phase response

$$F_{\mathrm{P}}^{(i)}(\tilde{\boldsymbol{\varepsilon}}) = 0.5 \sum_{j,k=1}^{K} \left| \exp\left(j\angle F_{jk}^{(i)} \right) - \exp\left(j\angle \overline{F}_{jk}^{(i)} \right) \right|^2$$

Jacobian Maps

Jacobian maps: cost function derivatives plotted vs. voxel location

- **magnitude maps**

$$\left.\frac{\partial F_{\mathrm{M}}^{(i)}}{\partial p_n}\right|_{p_n = \varepsilon_{r,n},\sigma_n} = \sum_{j,k=1}^{K} (|\, F_{jk}^{(i)} \,| - |\, \overline{F}_{jk}^{(i)} \,|) \frac{\partial \,|\, F_{jk}^{(i)} \,|}{\partial p_n} \qquad n = 1,\ldots,N \quad i = 1,\ldots,N_f$$

where

$$\frac{\partial \,|\, F \,|}{\partial p_n} = |\, F \,|^{-1} \cdot \left[\mathrm{Re}\, F \cdot \mathrm{Re}\left(\frac{\partial F}{\partial p_n} \right) + \mathrm{Im}\, F \cdot \mathrm{Im}\left(\frac{\partial F}{\partial p_n} \right) \right] \qquad F \equiv F_{jk}^{(i)}$$

- **phase maps**

$$\left.\frac{\partial F_{\mathrm{P}}^{(i)}}{\partial p_n}\right|_{p_n = \varepsilon_{r,n},\sigma_n} = \sum_{j,k=1}^{K} \sin\left(\angle F_{jk}^{(i)} - \angle \overline{F}_{jk}^{(i)} \right) \frac{\partial \angle F_{jk}^{(i)}}{\partial p} \qquad n = 1,\ldots,N \quad i = 1,\ldots,N_f$$

where

$$\frac{\partial \angle F}{\partial p_n} = |\, F \,|^{-2} \cdot \left[\mathrm{Re}\, F \cdot \mathrm{Im}\left(\frac{\partial F}{\partial p_n} \right) - \mathrm{Im}\, F \cdot \mathrm{Re}\left(\frac{\partial F}{\partial p_n} \right) \right]$$

Jacobian Maps: Summary

• magnitude vs. permittivity maps

$$M_{\varepsilon_r}^{(i)}(u,v) = \left.\frac{\partial F_{\mathrm{M}}^{(i)}}{\partial \varepsilon_{r,n}}\right|_{(u,v)}$$

• magnitude vs. conductivity maps

$$M_{\sigma}^{(i)}(u,v) = \left.\frac{\partial F_{\mathrm{M}}^{(i)}}{\partial \sigma_{n}}\right|_{(u,v)}$$

• phase vs. permittivity maps

$$P_{\varepsilon_r}^{(i)}(u,v) = \left.\frac{\partial F_{\mathrm{P}}^{(i)}}{\partial \varepsilon_{r,n}}\right|_{(u,v)}$$

• phase vs. conductivity maps

$$P_{\sigma}^{(i)}(u,v) = \left.\frac{\partial F_{\mathrm{P}}^{(i)}}{\partial \sigma_{n}}\right|_{(u,v)}$$

47

Example 1: Detecting Scatterer in a Homogeneous Lossy Dielectric

circular array of six probes: vertical polarization only

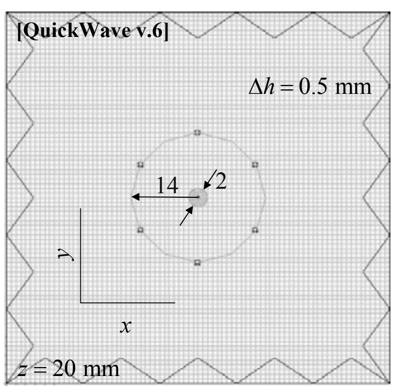

target structure #1
$(x_s, y_s) = (20, 20)$ mm

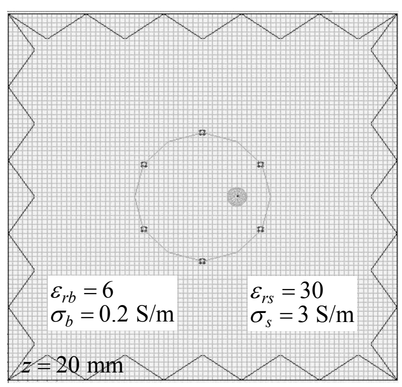

target structure #2
$(x_s, y_s) = (23.5, 20)$ mm

48

Example 1: Detecting Scatterer in a Homogeneous Lossy Dielectric

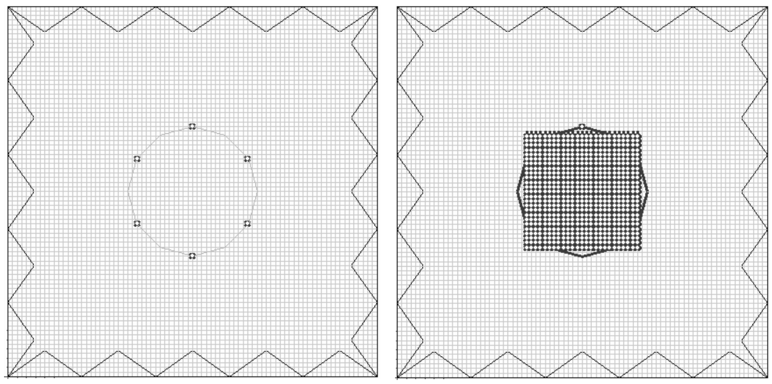

model structure:
background only

	true center		map minimum	
	x	*y*	*x*	*y*
case #1	20.00	20.00	20.00	20.00
case #2	23.50	20.00	23.00	20.00

Example 1: Detecting Scatterer in a Homogeneous Lossy Dielectric

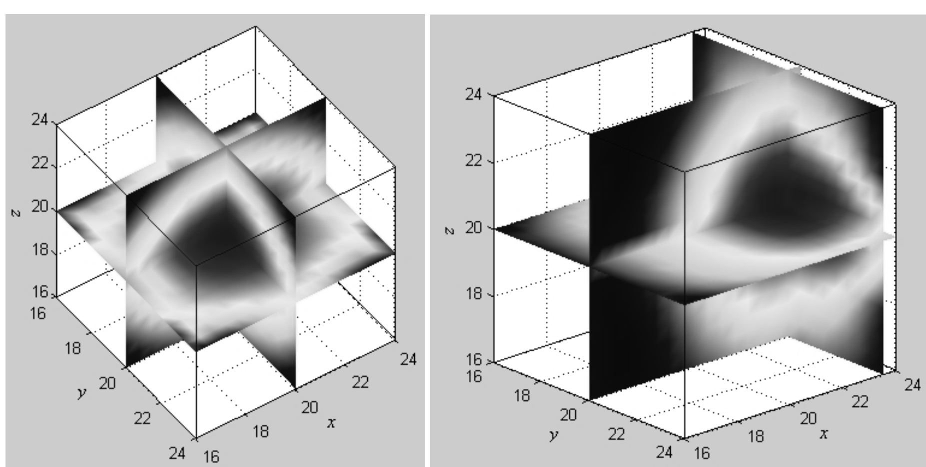

case #1　　case #2

Example 2: Detecting Scatterer in a Heterogeneous Lossy Dielectric

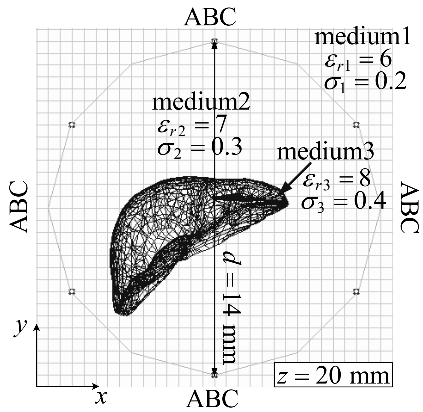

cross-section of
model structure:
background only

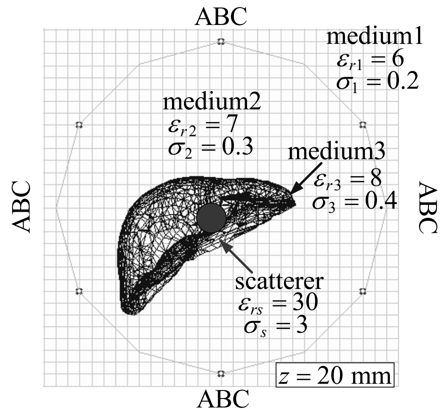

cross-section of
target structure

Example 2: Detecting Scatterer in a Heterogeneous Lossy Dielectric

data acquisition setup for a 3D scan

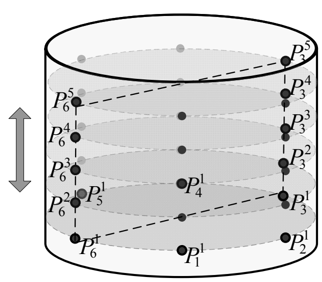

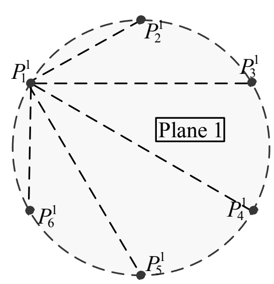

acquisition planes
are also planes where
Jacobian maps are
plotted

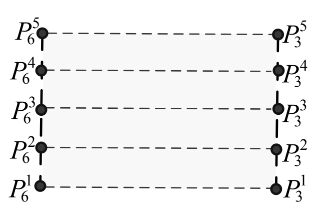

Example 2: Detecting Scatterer in a Heterogeneous Lossy Dielectric

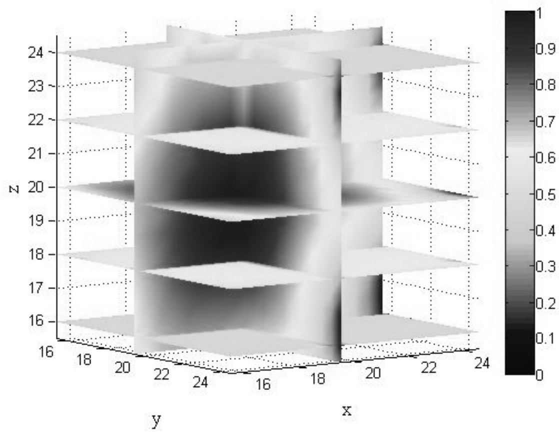

Location (x, y) (in mm) in the plane z = 20 mm	True Center	Map Minimum
	(19.00, 19.00)	(19.65, 19.73)

53

Summary

- response sensitivity analysis is crucial in design optimization and the solution of inverse problems
- the AVM is the most efficient method for SA – requires only additional 1 system analysis regardless of the number of parameters
- the self-adjoint method is applicable to network parameters – it does not require any additional system analyses
- numerically efficient – overhead is negligible compared to simulation time regardless of N
- reasonable memory even if N is on the order of 10^5
- versatile: applies to both shape and material parameters

54

References and Further Reading

1. L. Liu, A. Trehan, and N.K. Nikolova, “Near-field detection at microwave frequencies based on self-adjoint response sensitivity analysis,” *Inverse Problems*, submitted.
2. P. Zhao, M.H. Bakr, and N.K. Nikolova, “Adjoint first order sensitivities of transient responses and their applications in the solution of inverse problems,” *IEEE Trans. Antennas Propagat*., vol. 57, No. 7, pp. 2137–2146, July 2009.
3. N.K. Nikolova, X. Zhu, Y. Song, A. Hasib, and M.H. Bakr, “*S*-parameter sensitivities for electromagnetic optimization based on volume field solutions,” *IEEE Trans. Microwave Theory Tech*., Jun. 2009.
4. L. Vardapetyan, J. Manges, and Z. Cendes, “Sensitivity analysis of S-parameters including port variations using the transfinite element method,” *IEEE MTT-S Int. Microw. Symp. Dig*., Atlanta, GA, Jun. 2008, pp. 527–530.
5. Y. Song and N.K. Nikolova, “Memory efficient method for wideband self-adjoint sensitivity analysis,” *IEEE Trans. Microwave Theory Tech*., vol. 56, pp. 1917–1927, Aug. 2008.
6. D. Li, J. Zhu, N.K. Nikolova, M.H. Bakr, and J.W. Bandler, “Electromagnetic optimization using sensitivity analysis in the frequency domain,” *IET Microw. Antennas Propag*., vol. 1, pp. 852–859, Aug. 2007.
7. M. Swillam, M.H. Bakr, N.K. Nikolova, and X. Li, “Adjoint sensitivity analysis of dielectric discontinuities using FDTD,” *Electromagnetics*, vol. 27, pp. 123–140, Feb. 2007.
8. Q. Fang, P.M. Meaney, and K.D. Paulsen, “Singular value analysis of the Jacobian matrix in microwave image reconstruction,” IEEE Trans. Antennas Propagat., vol. 54, pp. 2371–2380, Aug. 2006.
9. S.M. Ali, N.K. Nikolova, and N.T. Sangary, “Near-field microwave nondestructive testing for defect shape and and material identification,” *Nondestructive Testing & Evaluation*, vol. 21, pp. 79–93, Jun. 2006.

References and Further Reading – 2

10. N.K. Nikolova, Ying Li, Yan Li, and M.H. Bakr, “Sensitivity analysis of scattering parameters with electromagnetic time-domain simulators,” *IEEE Trans. Microwave Theory Tech*., vol. 54, pp. 1598–1610, Apr. 2006.
11. N.K. Nikolova, J. Zhu, D. Li, M.H. Bakr, and J.W. Bandler, “Sensitivity analysis of network parameters with electromagnetic frequency-domain simulators,” *IEEE Trans. Microwave Theory Tech*., vol. 54, pp. 670–681, Feb. 2006.
12. Q. Fang, P.M. Meaney, S.D. Geimer, A. V. Streltsov, and K. D. Paulsen, “Microwave image reconstruction from 3-D fields coupled to 2-D parameter estimation,” *IEEE Trans. Medical Imaging*, vol. 23, pp. 475–484, Apr. 2004.
13. N.K. Nikolova, H.W. Tam, and M.H. Bakr, “Sensitivity analysis with the FDTD method on structured grids,” *IEEE Trans. Microwave Theory Tech*., vol. 52, pp. 1207–1216, Apr. 2004.
14. M.H. Bakr and N.K. Nikolova, “An adjoint variable method for frequency domain TLM problems with conducting boundaries,” *IEEE Microw. and Wireless Comp. Lett*., vol. 13, pp. 408–410, Sep. 2003.
15. H. Akel and J.P. Webb, “Design sensitivities for scattering-matrix calculation with tetrahedral edge elements,” *IEEE Trans. Magnetics*, vol. 36, pp. 1043–1046, Jul. 2000.
16. F. Azadivar, “A tutorial on simulation optimization,” *Proc. of the 24th Conference on Winter Simulation* (WSC 1992), ACM, Arlington, VA, Dec. 1992, pp. 198–204.
17. E.J. Haug, K.K. Choi and V. Komkov, *Design Sensitivity Analysis of Structural Systems*. Orlando: Academic Press Inc., 1986.
18. P. Neittaanmäki, M. Ridnicki, and S. Savini, *Inverse Problems and Optimal Design in Electricity and Magnetism*. Oxford: Clarendon Press, 1996.
19. A.D. Belegundu and T.R. Chandrupatla, *Optimization Concepts and Applications in Engineering*. Upper Saddle River, NJ: Prentice Hall, 1999.